J. Org. Chem. **1999,** *64,* 6401−6410

The Stability of Bridgehead Carbocations

José-Luis M. Abboud,*[,†] Marta Herreros,[†] Rafael Notario,[†] John S. Lomas,[‡] Jiri Mareda,[§]
Paul Müller,*[,§] and Jean-Claude Rossier[§]

*Instituto de Química Física, "Rocasolano", c/Serrano 119, E-28006 Madrid, Spain,
Institut de Topologie et de Dynamique des Systèmes (ITODYS), Université de Paris 7, associé au CNRS,
1 rue Guy de la Brosse, 75005 Paris, France, and Département de Chimie Organique,
Université de Genève, CH-1211 Genève 4, Switzerland*

Received April 29, 1999

The gas-phase stability of bridgehead carbocations has been determined by Fourier transform ion cyclotron resonance spectroscopy (FT ICR) based on dissociative proton attachment (DPA) of bridgehead bromides, chlorides, and alcohols. When appropriate leaving group corrections are applied, the relative ion stabilities obtained from these precursors are identical. The relative rate constants (log *k*) for solvolysis of bridgehead derivatives correlate with the stabilities of the cations over the entire reactivity range. Theoretical calculations of the stabilities of the ions relative to those of the respective hydrocarbons at the MP2/6-311G** level agree fully with the experimental data.

1. Introduction

In the past, most of the understanding of the structure and stability of carbenium ions was derived from the solvolytic reactivity of alkyl halides and carboxylate or sulfonate esters under S_N1 conditions.[1] Rough correlations between ionization data for the generation of carbenium ions from halide precursors in solution with the corresponding hydride affinities in the gas phase[2] and the correlation of Gibbs (free) energies of activation for solvolysis of halides with their enthalpies of ionization in solution[3] suggested structural and energetic similarities between carbenium ions and transition states for solvolysis. More recently, detailed experimental insight into the structure of carbenium ions became available by IR,[4] NMR,[5] and X-ray[6] investigations, and high-level ab initio calculations have been used to compute ^{13}C NMR shifts and geometries of cations with remarkable precision.[7] Energies of carbenium ions may also be calculated by these methods; however, the precision of the calculations is difficult to assess owing to the lack of experimental data.

In their pioneering investigation on bridgehead reactivity, Schleyer et al. were able to rationalize the rates of solvolysis of bridgehead derivatives in terms of the strain changes between bridgehead hydrocarbons and the corresponding carbenium ions, as calculated by molecular mechanics.[8] However, since the force field used was empirical and adjusted so as to produce the best possible fit with the rate data,[9] the relevance of the calculations with respect to the stability of carbenium ions is open to debate.

Over the past 7 years, we have obtained experimental data for the stabilities of bridgehead carbenium ions in the gas phase by several methods. A first set of data was obtained by measuring the gas-phase basicity of olefins or the equilibrium constants for bromide exchange between cations by ICR techniques.[10] More recently, Abboud et al. reported that dissociative proton attachment (DPA) may be used to generate carbenium ions from halides and alcohols under mild conditions and measure their stability.[11] This approach allowed measurements of ions as strained as the 1-norbornyl (1-bicyclo[2.2.1]-heptyl) or 6-tricyclo[3.2.1.0^{3,6}]octyl cations, which are not observable under ICR conditions.[12] Herein, we report the details of our DPA results obtained from bromides, chlorides, and alcohols over the full rate range of bridgehead solvolysis. The experimental ion stabilities are in perfect agreement with data obtained from ab initio calculations.

2. Dissociative Proton Attachment (DPA)

Protonation of a halide or an alcohol R−X in the gas phase produces ion−molecule complexes, which decay

---

* To whom correspondence should be addressed. (P.M.) Tel: +41 22 7026527. Fax: +41 22 3287396. E-mail: paul.muller@chiorg.unige.ch.

[†] "Rocasolano", Madrid.

[‡] ITODYS, Paris.

[§] University of Geneva.

(1) Bethell, D.; Gold, V. *Carbonium Ions*; Academic Press: New York, 1967. *Carbonium Ions, Vol. I−V*; Olah, G. A., Schleyer, P. v. R., Eds.; Wiley: New York, 1968−1976. Vogel, P. *Carbocation Chemistry*; Elsevier: New York, 1985.

(2) Arnett, E. M.; Pienta, N. J. *J. Am. Chem. Soc.* **1980**, *102*, 3329−3334.

(3) Arnett, E. M.; Petro, C.; Schleyer, P. v. R. *J. Am. Chem. Soc.* **1979**, *101*, 522−526.

(4) Sunko, D. E. In *Stable Carbocation Chemistry*; Prakash, G. K. S., Schleyer, P. v. R., Eds.; Wiley: New York, 1997; pp 349−388.

(5) Olah, G. A.; Prakash, G. K. S.; Sommer, S. *Superacids*; Wiley: New York, 1985; pp 65−175.

(6) Laube, T. *Acc. Chem. Res.* **1995**, *28*, 399−405.

(7) Schleyer, P. v. R.; Marker, C.; Buzek, P.; Sieber, S. In *Stable Carbocation Chemistry*; Prakash, G. K. S., Schleyer, P. v. R., Eds.; Wiley: New York, 1997; pp 19−74.

(8) Bingham, R. C.; Schleyer, P. v. R. *J. Am. Chem. Soc.* **1971**, *93*, 3189−3199. Parker, W.; Trauter, R. L.; Watt, C. I. F.; Chang, L. W. K.; Schleyer, P. v. R. *J. Am. Chem. Soc.* **1974**, *96*, 7121−7122.

(9) Müller, P.; Blanc, J.; Mareda, J. *Chimia* **1984,** *39*, 234; *Helv. Chim. Acta* **1986**, *69*, 635. Müller, P.; Mareda, J.; Milin, D. *J. Phys. Org. Chem.* **1995**, *8*, 507−528.

(10) Müller, P.; Milin, D.; Feng, W. Q.; Houriet, R.; Della, E. W. *J. Am. Chem. Soc.* **1992**, *114*, 6169−6172.

(11) Abboud, J.-L. M.; Notario, R.; Ballesteros, E.; Herreros, M.; Mó, O.; Yañez, M.; Elguero, J.; Boyer, G.; Claramunt, R. *J. Am. Chem. Soc.* **1994**, *116*, 2486−2492.

(12) Abboud, J.-L. M.; Castaño, O.; Della, E. W.; Herreros, M.; Müller, P.; Notario, R.; Rossier, J.-C. *J. Am. Chem. Soc.* **1997**, *119*, 2262−2266.

10.1021/jo990724x CCC: $18.00

almost without activation energy to free ions and HX. The FT ICR technique allows one to find the base B such that its conjugate acid BH^+ is just able to transfer a proton to R−X, according to (1), where X = OH or halogen.

$$R{-}X(g) + BH^+(g) \rightarrow R^+(g) + HX(g) + B(g) \quad (1)$$

The gas-phase basicity of the base B, GB(B) is defined as the standard Gibbs energy change for reaction 2, GB(B) = $\Delta G°_{(2)}$

$$BH^+(g) \rightarrow B(g) + H^+(g) \quad (2)$$

Reaction 3 decribes the halide or hydroxide ion exchange between two carbocations $R_1^+(g)$ and $R_2^+(g)$:

$$R_1^+(g) + R_2{-}X(g) \rightarrow R_2^+(g) + R_1{-}X(g) \quad \Delta G°_{(3)} \quad (3)$$

The $\Delta G°_{(3)}$ values allow the quantitative ranking of the stabilities of $R_1^+(g)$ and $R_2^+(g)$.[12,13]

If B_1 and B_2 are two bases defining the DPA onsets of $R_1X(g)$ and $R_2X(g)$ as determined under the same experimental conditions, then eq 4 holds:[12,13]

$$\Delta G°_{(3)} \approx GB(B_1) - GB(B_2) \quad (4)$$

This expression reduces the determination of the relative stabilities of $R_1^+(g)$ and $R_2^+(g)$, through the formal halide or hydroxide exchange (reaction 3), to that of the DPA threshold for the corresponding precursors (reaction 1).[11−13]

A very important feature of this technique is that carbocations are generated under extremely mild conditions and have much less tendency to rearrange than when generated by direct electron ionization, as in the standard ICR method.

3. Experimental Section

3.1. Synthesis of Halides and Alcohols. The synthesis of the bromide precursors was reported in our previous paper.[12] 1-Chloro[1]diadamantane (**3a**) and 1-hydroxy[1]diadamantane (**3b**) (1-hydroxyspiro[adamantane-2,2′-adamantane]) were obtained by the published procedures.[14,15] Bicyclo[3.3.3]undecane was synthesized from bicyclo[3.3.1]nonan-2-one as described in ref 16. It was converted to the 1-hydroxy derivative **4b** by oxidation with dimethyldioxirane.[17] The chloride **4a** was prepared from **4b** according to ref 8b. Ring expansion of bicyclo[3.3.1]nonan-9-one with diazomethane afforded bicyclo[3.3.2]decan-7-one, which was reduced to bicyclo[3.3.2]decane and functionalized at the bridgehead with either chromic acid or dimethyldioxirane[17] to yield 1-hydroxybicyclo[3.3.2]decane (**5b**), from which the chloride **5a** was obtained with $SOCl_2$.[18] 3-Chlorohomoadamantane (**6a**) was prepared via ring expansion of adamantane-1-carboxylic acid, via 3-homoadamananol (**6b**), which was converted to the chloride **6a** with $SOCl_2$.[19] Oxidative decarboxylation of 1-bicyclo[2.2.2]octane carboxylic acid[20] afforded 1-chlorobicyclo[2.2.2]octane (**10a**).[21] 1-Chlorobicyclo[2.2.1]heptane (**15a**) was prepared from 2-norbornanone.[22]

3.2. The FT ICR Spectrometer. The study was carried out on a modified Bruker CMS 47 FT ICR mass spectrometer[23] used in previous studies.[11−13,24] A detailed description is given in refs 11, 12, 23, and 24. Some modifications of the standard instrument were introduced. They are described in refs 13a and 24. The substantial field strength of the supraconducting magnet, 4.7 T, allows the monitoring of ion−molecule reactions for relatively long periods of time.

3.3. The DPA Experiment. The basic concepts of the method have been developed in refs 11−13 and are summarized above. In general, mixtures of R−X(g) and a reference base, B(g), are prepared. They are introduced into the high-vacuum section of the instrument and subjected to electron ionization (using nominal energies in the 10−13 eV range). Nominal presures of R−X(g) are in the $(1{-}3) \times 10^{-7}$ mbar range. Pressures of B are usually three to five times larger, depending on the system. Charged fragments (mostly from B) act as primary proton sources. In general, after 1−2 s the main ions present are $BH^+(g)$ and $R^+(g)$. After reaction times of ca. 5 s, all ions, with the exception of $BH^+(g)$, are ejected off the ICR cell by means of radio frequency ejection “chirps” (broad band).[25] Great care is taken to avoid the excitation of this ion, and for this purpose, use is made of an “ejection safety belt” (a feature of the Bruker software that strictly prevents the irradiation of a preselected frequency range around the resonance frequency of BH^+ in order to avoid its accidental excitation). $BH^+(g)$ is then allowed to react for times of up to 30 s. During this period of time, the main reactions observed are, first, the formation of $R^+(g)$ and, later on, that of the hydrogen-bonded dimers of B $(BHB)^+(g)$ and, finally, variable amounts of $(B{-}R)^+(g)$. The formation of $(BHB)^+(g)$ is frequently encountered in proton exchange studies. The formation of $(B{-}R)^+$ is a consequence of the electrophilicity of $R^+(g)$ and the stability of this ion with respect to proton transfer to B(g).

Given the very low pressures prevailing in these experiments, reaction 1 is essentially irreversible, the partial pressure of XH being very low and, while a true equilibrium is not reached, the onset of the process can be clearly observed. The experimental results of the study are presented in Table 1.

In our previous studies[12,13a] the gas-phase basicities of the reference bases B were expressed relative to NH_3, according to reaction 5, (GB(B) = $-\Delta G°_{(5)}$.

$$NH_4^+(g) + B(g) \rightarrow BH^+(g) + NH_3(g) \quad \Delta G°_{(5)} \quad (5)$$

The GB(B) values were from ref 26, and most of them originated in R. W. Taft’s laboratory. In this paper, we shall

---

(13) (a) Abboud, J.-L. M.; Castaño, O.; Herreros, M.; Elguero, J.; Jagerovic, N.; Notario, R.; Sak, K. *Int. J. Mass Spectrom. Ion Processes* **1998**, *175*, 35−40. (b) Abboud, J.-L.; Castaño, O.; Herreros, M.; Leito, I.; Notario, R.; Sak, K. *J. Org. Chem.* **1998**, *63*, 8995−8997.

(14) Graham, W. D.; Schleyer, P. v. R. *Tetrahedron Lett.* **1972**, 1179−1180; Sosnowski, J. J.; Rheingold, A. L.; Murray, R. K. *J. Org. Chem.* **1985**, *50*, 3788−3791.

(15) (a) Lomas, J. S.; D'Souza, M. J.; Kevill, D. N. *J. Am. Chem. Soc.* **1995**, *117*, 1126−1130. (b) Kevill, D. N.; D'Souza, M. J. D.; Lomas, J. S. *J. Chem. Soc., Perkin Trans. 2* **1997**, 131−132.

(16) Wayne, G. S.; Snyder, G. J. *Synth. Commun.* **1995**, *25*, 3267−3270.

(17) (a) Murray, R. W.; Jeyaraman, R.; Mohan, L. *J. Org. Chem.* **1985**, *50*, 2847−2472. (b) Müller, P.; Rossier, J.-C. Unpublished results.

(18) Bingham, R. C.; Schleyer, P. v. R. *J. Org. Chem.* **1971**, *36*, 1198−1201.

(19) Stetter, H.; Schwarz, M.; Hirschhorn A. *Chem. Ber.* **1959**, *92*, 1629−1635. Stetter, H.; Mayer, J.; Schwarz, M.; Wulff, K. *Chem. Ber.* **1960**, *93*, 226−230. Stetter, H.; Goebel, P. *Chem. Ber.* **1963**, *96*, 550−555.

(20) Grob, C. A.; Ohta, M.; Renk, E. Weiss, E. *Helv. Chim. Acta* **1958**, *41*, 1191−1197.

(21) Becker, K. B.; Geisel, M.; Grob, C. A.; Kuhnen, F. *Synthesis* **1973**, 493−494.

(22) Rieke, D.; Bales, S. E. *Org. Synth.* **1980**, *59*, 85−94.

(23) Laukien, F. H.; Allemann, M.; Bischofberger, P.; Grossmann, P. Kellerhals, H. P.; Kopfel, P. In *Fourier Transform Mass Spectrometry, Evolution, Innovation and Applications*; Buchanan, M. V., Ed.; ACS Symposium Series 359; American Chemical Society: Washington, DC, 1987; Chapter 5, p 81.

(24) Abboud, J.-L. M.; Herreros, M.; Notario, R.; Esseffar, M. Mó, O.; Yáñez, M. *J. Am. Chem. Soc.* **1996**, *118*, 1126−1130.

(25) Soo, O. G.; Buchanan, M. V.; Comisarov, M. R. In *Fourier Transform Mass Spectrometry, Evolution, Innovation, and Applications*; Buchanan, M. V., Ed.; ACS Symposium Series 359; American Chemical Society: Washington, DC, 1987; Chapter 1.

(26) Lias, S. G.; Bartmess, J. E.; Liebman, J. F.; Holmes, J. L.; Levin, R. D.; Mallard, W. G. NIST Standard Reference Database 19A, Computerized Version 1.1. Standard reference data, NIST, Gaithersburg, MD 20899, 1989.

Table 1. Experimentally Determined DPA Onsets for Reaction 1[a]

no.	compound	reference[b]	GB	reference[c]	GB	$\Delta G°_{H+}(g)$[d]	$\Delta G°_{(6)}$	Δlog *k*
1b	2-*tert*-butyladamantan-2-ol[e]	n-$C_4H_9NH_2$	211.9	$C_2H_5CON(CH_3)_2$	212.2	212.1	10.2	8.8
2b	9-*tert*-butylbicyclo[3.3.1]nonan-9-ol[e]	n-$C_3H_7NH_2$	211.3	n-$C_4H_9NH_2$	211.9	211.6	9.7	8.6
3a	1-chloro[1]diadamantane[f]	$CH_2{=}CHCH_2NH_2$	209.2	n-$C_3H_7NH_2$	211.3	210.3	16.7	7.7
3b	diadamantan-1-ol[f]	$CH_3CON(C_2H_5)_2$	213.8	$(CH_3)_2NH$	214.3	214.1	12.2	7.7
4a	1-chlorobicyclo[3.3.3]undecane[f]	$(t$-$C_4H_9)_2S$	206.5	c-$C_3H_5NH_2$	207.9	207.2	13.6	6.9
4b	bicyclo[3.3.3]undecan-1-ol[f]	*neo*-$C_5H_{11}NH_2$	213.7	$CH_3CON(C_2H_5)_2$	213.8	213.8	11.9	6.9
5a	1-chlorobicyclo[3.3.2]decane[f]	$(n$-$C_4H_9)_2S$	201.3	$(c-C_3H_5)_2CO$	203.3	202.3	8.7	3.5
5b	bicyclo[3.3.2]decan-1-ol[f]	isophorone	205.9	3-F-pyridine	208.0	207.0	5.1	3.5
6a	3-chlorohomoadamantane[f]	$(C_2H_5)_2S$	197.7	$(i$-$C_3H_7)_2O$	197.9	197.8	4.2	2.4
6b	3-homoadamantanol[f]	isophorone	205.9	$(t$-$C_4H_9)_2S$	206.5	206.2	4.3	2.4
7a	1-chloroadamantane[f]	$(C_2H_5)_2CO$	192.9	t-$C_4H_9OCH_3$	194.2	193.6	(0.0)	(0.0)
7b	1-adamantanol[f]	$(n$-$C_4H_9)_2S$	201.3	Pyrazine	202.4	201.9	(0.0)	(0.0)
7c	1-bromoadamantane[e]	$(C_2H_5)_2CO$	192.9	t-$C_4H_9OCH_3$	194.2	193.6	(0.0)	(0.0)
8a	2-*exo*-chloronorbornane[f,h]	$CH_3COC_2H_5$	190.1	$C_2H_5CO_2CH_3$	191.0	190.6	−3.0	−1.1
8c	2-*exo*-bromonorbornane[e]	$CH_3COC_2H_5$	190.1	$C_2H_5CO_2CH_3$	191.0	190.6	−3.0[h]	−1.1
9a	2-chloro-2-methylpropane[g]	t-C_4H_9SH	187.6	$CH_3CO_2CH_3$	189.0	188.3	−5.3	2.8
9c	2-bromo-2-methylpropane[e]						−5.3	2.8
10a	1-chlorobicyclo[2.2.2]octane[f]	c-C_3H_5CN	185.8	t-C_4H_9CN	186.5	186.2	−7.4	−3.6
10c	1-bromobicyclo[2.2.2]octane[e]	i-C_3H_7CN	184.7	$HCO_2(n$-$C_3H_7)$	185.0	184.9	−8.7	−3.6
11c	4-bromohomocubane[e]						−11.2	−5.9
12c	bromocubane[e]						−16.4	−7.3
13c	3-bromonoradamantane[e]	CH_3CHO	176.0	CH_3SH	177.3	176.7	−16.9	−6.9
14c	1-bromohomocubane[e]						−26.7	−11.0
15a	1-chloronorbornane[f]	Cl_3CCN	165.5	Cl_3CCH_2OH	167.0	166.3	−27.3	−10.1
15c	1-bromonorbornane[e]	Cl_3CCN	165.5	Cl_3CCH_2OH	167.0	166.3	−27.3	−10.1
16c	6-bromotricyclo[3.2.1.$0^{3,8}$]octane[e]	$(CF_3CH_2)_2O$	161.3	H_2CO	163.3	162.3	−31.3	−13.9

[a] All values in kcal mol^{-1}. [b] Strongest base *able to lead* to DPA. [c] Weakest base *not leading* to DPA. [d] Average of the two (GB) values. [e] From ref 12. [f] This work. [g] From ref 13b. [h] The value obtained by direct exchange was −3.0 ± 0.3 kcal mol^{-1}.

use data from the major critical revision and compilation of gas-phase basicities and proton affinities recently published by Lias and Hunter,[27] which significantly updates the values given in ref 26. In Table 1, we present the DPA onsets as given by $\Delta G°_{H+}(g)$, the average of the GB values for the *strongest base able to lead to DPA, and the weakest base not leading to DPA*. Notice that now these values do not refer to reaction 5, but are “absolute values”, as defined by reaction 2. For the sake of self-consistency, the experimental onsets reported in ref 12 were also anchored to this updated gas-phase basicity scale and are also given in Table 1. The experimental uncertainties in the individual DPA onsets are estimated to be ca. 2 kcal mol^{-1}. Notice that some $\Delta G°_{(6)}$ values in ref 12 were obtained by direct bromide exchange between a bridgehead bromide and a cation generated by DPA. The corresponding values have therefore been revised according to the new reference GB values given in ref 27.

3.4. Computational Methods. Geometries of carbocation and corresponding hydrocarbon structures were fully optimized at the Møller−Plesset[28] level of theory using the 6-311G** basis set.[29] Computations were carried out with Gaussian-92[30] and Gaussian-94[31] systems of programs. Møller−Plesset perturbation theory to the second order (MP2) is often used to incorporate the effects of electron correlation in the post-SCF computational methods. The importance of electron correlation to correctly describe carbocations is now well established.[32] The MP2 computations successfully reproduce experimentally obtained energies, spectral properties and structures, for various carbocations.[32b,33] The geometry optimizations at the MP2 level were extended from carbocations to the corresponding hydrocarbons.

The geometry optimizations at the correlated level were limited to carbocations and the corresponding hydrocarbons containing up to 11 non-hydrogen atoms. Consequently, the 2-*tert*-butyladamant-2-yl and 9-*tert*-butylbicyclo[3.3.1]non-9-yl cations and their derivatives were fully optimized at the HF/6-31G* level.[33a,34] The geometry optimizations of chlorides, bromides and alcohols were also performed using the HF/6-31G* method. In general, this level of theory is considered appropriate for such uncharged species.[35]

The total electronic energies for carbocations and the corresponding hydrocarbons were computed at the MP2/6-311G** level to permit the evaluation of the hydride exchange between the cation and adamantane. Leaving group corrections for the conversion of data for chlorides and alcohols into those for bromides and hydrocarbons, respectively, are based on the energies computed at the HF/6-31G* level. The thermochemical parameters necessary to calculate enthalpies and

---

(27) Hunter, E. P. L.; Lias, S. G. *J. Phys. Chem. Ref. Data* **1998**, *27*, 413−656.

(28) Møller, C.; Plesset, M. S. *Phys. Rev.* **1934**, *46* 618−622. Head-Gordon, M.; Pople, J. A.; Frisch, M. J. *Chem. Phys. Lett.* **1988**, *153*, 503−506. Frisch, M. J.; M. Head-Gordon M.; Pople, J. A. *Chem. Phys. Lett.* **1990**, *166*, 275−280. Frisch, M. J., Head-Gordon, M.; Pople, J. A. *Chem. Phys. Lett.* **1990**, *166*, 281−289.

(29) Krishnan, R.; Binkley, J. S.; Seeger, R.; Pople, J. A. *J. Chem. Phys.* **1980**, *72*, 650−654. McLean A. D.; Chandler, G. S. *J. Chem. Phys.* **1980**, *72*, 5639−5648.

(30) Frisch, M. J.; Trucks, G. W.; Head-Gordon, M.; Gill, P. M. W.; Wong, M. W.; Foresman, J. B.; Johnson, B. G.; Schlegel, H. B.; Robb, M. A.; Replogle, E. S.; Gomperts, R.; Andres, J. L.; Raghavachari, K.; Binkley, J. S.; Gonzalez, C.; Martin, R. L.; Fox, J.; Defrees, D. J.; Baker, J.; Stewart J. J. P.; Pople, J. A. *Gaussian 92*, Gaussian Inc.; Pittsburgh, PA, 1992.

(31) Frisch, M. J.; Trucks, G. W.; Schlegel, H. B.; Gill, P. M. W.; Johnson, B. G.; Robb, M. A.; Cheeseman, J. R.; Keith, T. A.; Petersson, G. A.; Montgomery, J. A.; Raghavachari, K.; Al-Laham, M. A.; Zakrzewski, V. G.; Ortiz, J. V.; Foresman, J. B.; Cioslowski, J.; Stefanov, B. B.; Nanayakkara, A.; Challacombe, M.; Peng, C. Y.; Ayala, P. Y.; Chen, W.; Wong, M. W.; Andres, J. L.; Replogle, E. S.; Gomperts, R.; Martin, R. L.; Fox, D. J.;. Binkley, J. S.; Defrees, D. J.; Baker, J.; Stewart, J. P.; Head-Gordon, M.; Gonzalez M. C.; Pople, J. A. *Gaussian 94*; Gaussian Inc.: Pittsburgh, PA, 1995.

(32) (a) Sieber, S.; Schleyer, P. v. R.; Vancik, H.; Mesic, M.; Sunko, D. E. *Angew. Chem., Int. Ed. Engl.* **1993**, *32*, 1604−1606. Schleyer, P. v. R.; Carneiro, J. W. d. M.; Koch, W.; Forsyth, D. A. *J. Am. Chem. Soc.* **1991**, *113*, 3990−3992. (b) Sieber, S.; Buzek, P.; Schleyer, P. v. R.; Koch, W.; Carneiro, J. W. d. M. *J. Am. Chem. Soc.* **1993**, *115*, 259−270. (c) Gobbi, A.; Frenking, G. *J. Am. Chem. Soc.* **1994**, *116*, 9275−9286. Gobbi, A.; Frenking, G. *J. Am. Chem. Soc.* **1994**, *116*, 9287−9293.

(33) (a) Koch, W.; Liu, B.; DeFrees, D. J. *J. Am. Chem. Soc.* **1989**, *111*, 1527−1528. (b) Koch, W.; Liu, B.; DeFrees, D. J.; Sunko, D. E.; Vancik, H. *Angew. Chem., Int. Ed. Engl.* **1990**, *29*, 183−185. (c) Schleyer; P. v. R.; Sieber, S. *Angew. Chem., Int. Ed. Engl.* **1993**, *32*, 1606−1608. (d) Prakash, G. K. S., Schleyer, P. v. R., Eds. *Stable Carbocation Chemistry*; Wiley: New York, 1997. (e) Schleyer, P. v. R.; Maerker, C. *Pure Appl. Chem.* **1995**, *67*, 755−760.

(34) Petersson G. A.; Al-Laham, M. A. *J. Chem. Phys.* **1991**, *94*, 6081−690.

(35) Hehre, W. J.; Radom, L.; Schleyer, P. v. R.; Pople, J. A. *Ab Initio Molecular Orbital Theory*; Wiley: New York, 1986.

Table 2. Total Energies at HF/6-31G* and MP2/6-31G Levels, Zero-Point Vibrational Energies (ZPE), Thermal Corrections to Enthalpies (TCE), and Total Entropy Values (*S*) for Species Studied in This Work**

no.	compound	HF/6-31G*[a]	MP2/6-311G**[a]	ZPE[a,c,d]	TCE[a,d]	S[b,d,e]
1b	2-*tert*-butyl-2-adamantanol	−618.98854		0.38827	0.40126	103.8
1d	2-*tert*-butyladamantane	−544.14380		0.38279	0.39509	102.1
1e	2-*tert*-butyladamantanyl	−543.32437		0.36917	0.38217	107.0
2b	9-*tert*-butylbicyclo[3.3.1]nonanol	−581.10227		0.38034	0.39385	106.2
2d	9-*tert*-butylbicyclo[3.3.1]nonane	−506.25786		0.37472	0.38757	104.3
2e	9-*tert*-butylbicyclo[3.3.1]nonyl	−505.43768		0.36094	0.37455	109.4
4a	1-chlorobicyclo[3.3.3]undecane	−887.08268		0.30605	0.31712	94.2
4b	bicyclo[3.3.3]undecan-1-ol	−503.03196		0.32052	0.33145	92.5
4c	1-bromobicyclo[3.3.3]undecane	−2997.49247		0.30544	0.31681	97.0
4d	bicyclo[3.3.3]undecane	−428.17907	−429.93473	0.31598	0.32592	86.3
4e	1-bicyclo[3.3.3]undecyl	−427.35559	−429.06135	0.30231	0.31234	86.6
5a	1-chlorobicyclo [3.3.2]decane	−848.06033		0.27467	0.28423	90.4
5b	bicyclo[3.3.2]decan-1-ol	−464.00927		0.28909	0.29855	88.8
5c	1-bromobicyclo[3.3.2]decane	−2958.47042		0.27406	0.28390	93.1
5d	bicyclo[3.3.2]decane	−389.15469	−390.74472	0.28442	0.29286	81.8
5e	1-bicyclo[3.3.2]decyl	−388.31962	−389.86331	0.27135	0.27997	85.3
6a	3-chlorohomoadamantane	−885.95199		0.28264	0.29259	93.1
6b	3-homoadamantanol	−501.90041		0.29704	0.30690	91.8
6c	3-bromohomoadamantane	−2996.36181		0.28204	0.29225	95.7
6d	homoadamantane	−427.04557	−428.77489	0.29246	0.30126	85.9
6e	3-homoadamantyl	−426.20883	−427.89084	0.27931	0.28820	87.2
7a	1-chloroadamantane	−846.93583		0.25150	0.26004	83.9
7b	1-adamantanol	−462.88290		0.26581	0.27432	82.4
7c	1-bromoadamantane	−2957.34509		0.25089	0.25970	86.6
7d	adamantane	−388.02648	−389.59273	0.26134	0.26873	74.9
7e	1-adamantyl	−387.18030	−388.70501	0.24821	0.25576	78.1
8a	2-*exo*-chloronorbornane	−730.96646		0.18069	0.18788	80.5
8c	2-*exo*-bromonorbornane	−2841.37528		0.18002	0.18742	83.1
8e	2-norbornyl	−271.20061	−272.26910	0.17619	0.18286	76.8
9a	2-chloro-2-methylpropane	−616.20588		0.13136	0.13848	74.5
9c	2-bromo-2-methylpropane	−2726.61485		0.13082	0.13813	77.2
9d	2-methylpropane	−157.29898	−157.96418	0.14078	0.14715	69.0
9e	*tert*-butyl	−156.44255	−157.05658	0.11791	0.12504	75.7
10a	1-chlorobicyclo[2.2.2]octane	−770.01211		0.21177	0.22026	85.9
10c	1-bromobicyclo[2.2.2]octane	−2880.42114		0.21118	0.21990	87.9
10d	bicyclo[2.2.2]octane	−311.10360	−312.36649	0.22150	0.22889	79.7
10e	bicyclo[2.2.2]octyl	−310.24649	−311.46450	0.20846	0.21597	78.6
11c	4-bromohomocubane	−2915.82122		0.16717	0.17424	82.4
11d	homocubane	−346.50449	−347.85936	0.17755	0.18312	72.4
11e	4-homocubyl	−345.62349	−346.94795	0.16286	0.16896	74.3
12c	bromocubane	−2876.71058		0.13448	0.14095	77.4
12d	cubane	−307.39391	−308.58061	0.14480	0.14983	64.7
12e	cubyl	−306.50759	−307.66556	0.12982	0.13517	68.3
13c	3-bromonoradamantane	−2918.28560		0.21911	0.22712	85.6
13d	noradamantane	−348.97007	−350.37657	0.22960	0.23620	76.4
13e	3-noradamantyl	−348.10117	−349.46181	0.21574	0.22267	77.6
14c	1-bromohomocubane	−2915.81944		0.16710	0.17411	81.9
14e	1-homocubyl	−345.61517	−346.92458	0.16348	0.16938	73.4
15a	1-chloronorbornane	−730.96841		0.18028	0.18755	80.2
15c	1-bromonorbornane	−2841.37667		0.17966	0.18717	83.0
15d	norbornane	−272.06120	−273.16434	0.19002	0.19621	72.4
15e	1-norbonyl	−271.18117	−272.23517	0.17660	0.18310	74.9
16c	6-bromotricyclo[3.2.1.0^{3,6}]octane	−2879.21771		0.18640	0.19387	83.1
16d	tricyclo[3.2.1.0^{3,6}]octane	−309.90313	−311.14617	0.19679	0.20285	73.7
16e	6-tricyclo[3.2.1.0^{3,6}]octyl	−309.01119	−310.20579	0.18301	0.18945	74.9

[a] In hartrees. [b] In cal mol^{-1} K^{-1}. [c] ZPE values corrected by a factor of 0.9135 (ref 35). [d] Computed at HF/6-31G* level. [e] Corrected by symmetry number.

Gibbs free energies were obtained from harmonic vibrational frequency calculations at the HF/6-31G* level by using analytic-second derivative methods.[36] In particular, the zero-point energy (ZPE), thermal energy correction to the enthalpy (TCE) and entropy (S) were obtained from the vibrational frequency analysis. These values are listed in Tables 2 and 3 together with the total electronic energies.

Enthalpies and Gibbs free energies are based on the total electronic energies computed at the HF/6-31G* and MP2/6-311G** levels and on the thermochemical data listed in Table 2. To this end, the zero-point energy was added to the total electronic energy in order to account for the effects of molecular vibrations at 0 K. Thermal energy correction to the enthalpy was also applied in order to establish the energy of the system at 298.15 K. The entropy correction was scaled by a factor of 0.9135 to eliminate known systematic errors for computed frequencies.[35] The unscaled entropy data were corrected using the appropriate symmetry numbers.[37] Enthalpies (*E*) and Gibbs free energies (*G*) at 298.15 K derived from ab initio results are listed in Table 3.

For the 1-diadamantyl cation and its derivatives, which contain 20 non-hydrogen atoms, the total energies and vibra-

---

(36) Pople, J. A.; Krishnan, R.; Schlegel H. B.; Binkley, J. S. *Int. J. Quantum Chem. Symp.* **1979**, *13*, 325. Pople, J. A.; Krishnan, R.; Schlegel, H. B.; DeFrees, D.; Binkley, J. S.; Frisch, M. J.; Whiteside, R. F.; Hout, R. F.; Hehre, W. J. *Int. J. Quant Chem. Symp.* **1985**, *15*, 269−275.

(37) Stull, D. R.; Westrum, E. F.; Sinke, G. C. *The Chemical Thermodynamics of Organic Compounds*; Wiley: New York, 1969; Chapter 4.

Table 3. Enthalpies (*H*) and Free Energies (*G*) Derived from Total Electronic Energies Computed at the HF/6-31G* and MP2/6-311G Levels**

		HF/6-31G*		MP2/6-311G**	
no.	compound	$H^{a,b}$	$G^{a,b}$	$H^{a,b}$	$G^{a,b}$
1b	2-*tert*-butyl-2-adamantanol	−618.62087	−618.67020		
1d	2-*tert*-butyladamantane	−543.78182	−543.83032		
1e	2-*tert*-butyladamantanyl	−542.97414	−543.02497		
2b	9-*tert*-butylbicyclo[3.3.1]nonanol	−580.74131	−580.79175		
2d	9-*tert*-butylbicyclo[3.3.1]nonane	−505.90270	−505.95223		
2e	9-*tert*-butylbicyclo[3.3.1]nonyl	−505.09435	−505.14634		
4a	1-chlorobicyclo[3.3.3]undecane	−886.79204	−886.83680		
4b	bicyclo[3.3.3]undecan-1-ol	−502.72823	−502.77218		
4c	1-bromobicyclo[3.3.3] undecane	−2997.20208	−2997.24817		
4d	bicyclo[3.3.3]undecane	−427.88048	−427.92149	−429.63614	−429.67715
4e	1-bicyclo[3.3.3]undecyl	−427.06939	−427.11054	−428.77516	−428.81630
5a	1-chlorobicyclo [3.3.2]decane	−847.79986	−847.84281		
5b	bicyclo[3.3.2]decan-1-ol	−463.73572	−463.77791		
5c	1-bromobicyclo[3.3.2]decane	−2958.21022	−2958.25448		
5d	bicyclo[3.3.2]decane	−388.88643	−244.02974	−390.47647	−245.02750
5e	1-bicyclo[3.3.2]decyl	−388.06312	−388.10365	−389.60680	−389.64734
6a	3-chlorohomoadamantane	−885.68385	−885.72809		
6b	3-homoadamantanol	−501.61920	−501.66281		
6c	3-bromohomoadamantane	−2996.09396	−2996.13943		
6d	homoadamantane	−426.76961	−426.81042	−428.49893	−428.53973
6e	3-homoadamantyl	−425.94479	−425.98620	−427.62680	−427.66821
7a	1-chloroadamantane	−846.69755	−846.73739		
7b	1-adamantanol	−462.63158	−462.67073		
7c	1-bromoadamantane	−2957.10709	−2957.14824		
7d	adamantane	−387.78035	−387.81594	−389.34661	−389.38219
7e	1-adamantyl	−386.94602	−386.98313	−388.47072	−388.50783
8a	2-*exo*-chloronorbornane	−730.79421	−730.83243		
8c	2-*exo*-bromonorbornane	−2841.20343	−2841.24293		
8e	2-norbornyl	−271.03299	−271.06950	−272.10148	−272.13798
9a	2-chloro-2-methylpropane	−616.07876	−616.11416		
9c	2-bromo-2-methylpropane	−2726.48804	−2726.52469		
9d	2-methylpropane	−157.16401	−157.19679	−157.82920	−157.86199
9e	*tert*-butyl	−156.32771	−156.36365	−156.93521	−156.97116
10a	1-chlorobicyclo[2.2.2]octane	−769.81018	−769.85099		
10c	1-bromobicyclo[2.2.2]octane	−2880.21951	−2880.26127		
10d	bicyclo[2.2.2]octane	−310.89387	−310.93174	−312.15676	−312.19463
10e	bicyclo[2.2.2]octyl	−310.04856	−310.08590	−311.26656	−311.30391
11c	4-bromohomocubane	−2915.66144	−2915.70057		
11d	homocubane	−346.33673	−346.37114	−347.69161	−347.72602
11e	4-homocubyl	−345.46862	−345.50391	−346.79309	−346.82838
12c	bromocubane	−2876.58127	−2876.61804		
12d	cubane	−307.25660	−307.28734	−308.44330	−308.47404
12e	cubyl	−306.38365	−306.41610	−307.54162	−307.57408
13c	3-bromonoradamantane	−2918.07743	−2918.11808		
13d	noradamantane	−348.75373	−348.79003	−350.16023	−350.19652
13e	3-noradamantyl	−347.89716	−347.93404	−349.25780	−349.29468
14c	1-bromohomocubane	−2915.65978	−2915.69869		
14e	1-homocubyl	−345.45993	−345.49481	−346.76934	−346.80422
15a	1-chloronorbornane	−730.79645	−730.83455		
15c	1-bromonorbornane	−2841.20504	−2841.24447		
15d	norbornane	−271.88143	−271.91583	−272.98457	−273.01897
15e	1-norbonyl	−271.01334	−271.04894	−272.06734	−272.10294
16c	6-bromotricyclo[3.2.1.0^{3,6}]octane	−2879.03997	−2879.07943		
16d	tricyclo[3.2.1.0^{3,6}]octane	−309.71730	−309.75231	−310.96035	−310.99535
16e	6-tricyclo[3.2.1.0^{3,6}]octyl	−308.83757	−308.87314	−310.03217	−310.06775

[a] In Hartree at 298 K. [b] Aall thermochemical parameters computed at HF/6-31G* (see Table 2a).

tional frequency analysis were computed at the semiempirical level with the AM1 Hamiltonian.[38]

Discussion

4.1. DPA for Chlorides and Rates of Solvolysis. For the sake of consistency with our previous study,[12] cation stabilities are expressed relative to the 1-adamantyl cation (Ad$^+$) by means of eq 6. Data have been obtained for X = Cl, X = OH, and X = Br. The relevant quantity is $\Delta G°_{(6)}$ (see Table 1):

$$\mathrm{R}^+(\mathrm{g}) + \mathrm{Ad{-}X}(\mathrm{g}) \rightarrow \mathrm{R{-}X} + \mathrm{Ad}^+(\mathrm{g}) \quad \Delta G°_{(6)} \qquad (6)$$

The correlation between the standardized rate constants for the solvolysis of bridgehead derivatives, Δlog *k* (rate constants relative to 1-adamantyl-*p*-toluenesulfonate in 80% EtOH at 70°[39] and $\Delta G°(\mathrm{X} = \mathrm{Br})$ has been reported in a previous paper.[12] These rate constants have been extrapolated from a variety of different sources with different leaving groups and solvents and at differ-

---

[38] Dewar, M. J. S.; Zoebisch, E. G.; Healy, E. F. *J. Am. Chem. Soc.* **1985**, *107*, 3902−3909; Dewar, M. J. S.; Reynolds, C. H. *J. Comput. Chem.* **1986**, *2*, 140.

[39] Müller, P.; Milin, D. *Helv. Chim. Acta* **1991**, *74*, 1808−1816.

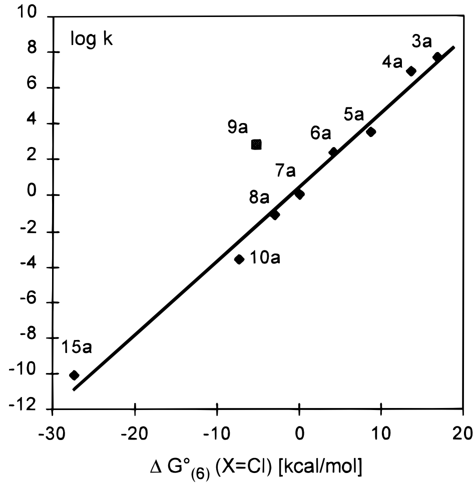

Figure 1. Plot of log *k* for solvolysis of bridgehead derivatives relative to 1-chloroadamantane vs experimental standard Gibbs energy change for chloride exchange in the gas phase, reaction 6. Log $k = 0.42\Delta G^\circ_{(6)}(X = Cl) + 0.43$. $r^2 = 0.9875$; $\sigma = 0.70$. *tert*-Butyl chloride (**9**-Cl) excluded from correlation. Data from Table 1.

ent temperatures by means of appropriate conversion factors or linear free energy correlations.[40,41] The datum for diadamantane was extrapolated from 1-chloro[1]-diadamantane (**3a**) solvolysis in EtOH at 25 °C, relative to 1-chloroadamantane ($k_{rel} = 1.7 \times 10^8$ s^{-1})[15] by means of the Arrhenius equation. The relative rate constants in other solvents are lower by a factor of ca. 3, which probably arises from the various extrapolations of the data collected at different temperatures. However, these variations are negligible considering the range of ca. 20 log units in rates. In Figure 1 the rate constants are plotted vs $\Delta G^\circ_{(6)}(X = Cl)$.

As Figure 1 shows, the rate constants of bridgehead chlorides correlate well ($r^2 = 0.9875$) with the gas-phase stabilities of the respective carbenium ions. *tert*-Butyl chloride (**9a**) deviates significantly from the plot, as expected from the behavior of the bromide (see below). The bridgehead chlorides investigated in this study extend the rate range of the reported correlation for bromides by ca. 8 log units by including compounds such as the diadamantyl and manxyl derivatives, **3a** and **4a**, respectively. The similarity of the slope of the plot in Figure 1 (slope = 0.415) with that reported for the correlation of log *k* with the DPA data of bromides (slope = 0.492) suggests that DPA data determined for different leaving groups should be identical after appropriate leaving group corrections. This should result in a unified scale for the stability of bridgehead carbenium ions.

4.2. DPA for Bromides, Chlorides, and Alcohols. For practical reasons, most of the DPA data have been obtained with bromides and are expressed relative to 1-bromoadamantane (**7c**) as reference compound. Chlorides and alcohols can be used for the same purpose, the reference compounds being 1-chloroadamantane (Ad-Cl, **7a**) and 1-adamantanol (Ad-OH, **7b**), respectively. In this study, we have determined experimental DPA values for the less reactive species from both bromo and chloro derivatives. Chlorides and alcohols were investigated in the case of highly reactive compounds. For both types of derivatives, the experimental DPA data of $\Delta G^\circ_{(6)}(X = Cl$ or $OH)$ have been corrected by $\Delta G^\circ_{(6a)}$ and $\Delta G^\circ_{(6b)}$ values, respectively, to yield the corresponding values for $\Delta G^\circ_{(6)}$(X = Br, calcd Cl) and $\Delta G^\circ_{(6)}$(X = Br, calcd OH). $\Delta G^\circ_{(6a)}$ and $\Delta G^\circ_{(6b)}$ were calculated at the HF/6-31G* level, except for the diadamantane derivatives (**3a**,**b**), for which AM1 calculations were used (see Table 4).

$$\text{Ad}-\text{Br(g)} + \text{R}-\text{Cl(g)} \rightarrow \text{Ad}-\text{Cl(g)} + \text{R}-\text{Br} \quad \Delta G^\circ_{(6a)} \qquad (6a)$$

$$\text{Ad}-\text{Br (g)} + \text{R}-\text{OH(g)} \rightarrow \text{Ad}-\text{OH(g)} + \text{R}-\text{Br} \quad \Delta G^\circ_{(6b)} \qquad (6b)$$

The leaving group corrections are generally small in the series of bridgehead derivatives, in particular when small bridges are involved, as in the case of the norbornyl or bicyclo[2.2.2]octyl derivatives. Substantial leaving group corrections are observed with 2-*tert*-butyladamant-2-yl (**1**), 9-*tert*-butylbicyclo[3.3.1]non-9-yl (**2b**), and [1]-diadamantyl (**3**). Large values suggest the presence of F-strain,[42,43] i.e., steric interactions between the leaving group and the molecular skeleton. The reactivity scale for bridgehead solvolysis is based on the assumption of negligible F-strain contributions within the series. However, the occurrence of F-strain in **3a** has been demonstrated conclusively.[15b] Fortunately, it is of no consequence in this study, because the rate constant for solvolysis and the DPA value have been determined with **3a**, using chloride as the leaving group, and F-strain should affect both values in a similar manner.

Figure 2 shows a comparison of the DPA data obtained with compounds for which either bromides and chlorides or chlorides and alcohols are available. The leaving group correction according to eq 6a is applied to the experimental data determined with chlorides to yield calculated values for bromides, $\Delta G^\circ_{(6)}$(X = Br, calcd Cl). These data are plotted vs the experimental DPA data for bromides $\Delta G^\circ_{(6)}(X = Br)$ *and* values calculated from DPA data of alcohols (after application of the leaving group correction, eq 6b), $\Delta G^\circ_{(6)}$(X = Br, calcd OH). The quality of the correlation is excellent (slope = 0.998, $r^2 = 0.9924$, $\sigma = 1.142$). These results strongly support the self-consistency of the approach. The slope of 0.998 implies that the ranking of the gas-phase carbocation stabilities obtained from chlorides, alcohols, and bromides is essentially identical for the compounds studied. Inspection of Figure 2 reveals that the case of the substituted diadamantyl derivatives (**3**) is by far the most unfavorable. This is so because the AM1 method is unlikely to provide an appropriate correction for the large differences in F-strain in these compounds,[15] even if isodesmic reactions are used. The large number of atoms of the diadamantane derivatives, however, precluded the use of higher computational levels. We consider, therefore, that in the case of **3** the uncertainty in the corrected $\Delta G^\circ_{(6)}(X = Br)$ values is of the order of 2−3 kcal mol^{-1}, and for this reason the datum for **3** is not included in the correlation shown in Figure 2.

---

[40] Bentley, T. W.; Roberts, K. *J. Org. Chem.* **1985**, *50*, 5852−5855. Bentley, T. W.; Christl, M.; Norman, S. *J. Org. Chem.* **1991**, *56*, 6238−6240.

[41] Müller, P.; Blanc, J.; Mareda, J. *Chimia* **1987**, *41*, 399−401.

[42] Brown, H. C. *J. Chem. Educ.* **1959**, *36*, 424. Slutsky, J.; Bingham, R. C.; Schleyer, P. v. R.; Dickason, W. C.; Brown, H. C. *J. Am. Chem. Soc.* **1970**, *96*, 1969−1970.

[43] Ohga, Y.; Munakata, M.; Kitagawa, T.; Kinoshita, T.; Takeuchi, K.; Oishi, Y.; Fujimoto, H. *J. Org. Chem.* **1994**, *59*, 4056−4067.

Table 4. Experimental and Theoretical Data for Gas-Phase and Solution Reactions[a]

no.	compound, R	$\Delta G^\circ_{(6a)}$ (Cl→Br)	$\Delta G^\circ_{(6b)}$ (OH→Br)	$\Delta G^\circ_{(6)}$(X = Br)[c] (calcd Cl)	$\Delta G^\circ_{(6)}$(X = Br)[d] (calcd OH)	$\Delta G^\circ_{(6)}$(X = Br,avg)	$\Delta G^\circ_{(6c)}$ (Br→H)	$\Delta G^\circ_{(7)}$ (exptl)	$\Delta G^\circ_{(7)}$ (theor)
1	2-*tert*-butyladamant-2-yl		5.7		15.9	15.9			17.2[e]
2	9-*tert*-butylbicyclo[3.3.1]non-9-yl		5.6		15.3	15.3			16.9[e]
3	[1]diadamantyl[b]	1.9[f]	5.9[f]	18.6[f]	18.1[f]	18.3[f]	−11.7[f]	6.6[f]	8.6[f]
4	1-bicyclo[3.3.3]undecyl[b]	−0.3	1.0	13.3	12.9	13.1	−3.5	9.5	8.5
5	1-bicyclo[3.3.2]decyl[b]	−0.5	0.6	8.2	5.7	6.9	−2.0	5.0	4.0
6	3-homoadamantyl[b]	−0.3	0.6	3.9	4.9	4.4	−2.1	2.3	1.8
7	1-adamantyl	(0.0)	(0.0)	(0.0)	(0.0)	(0.0)	(0.0)	(0.0)	(0.0)
8	2-*exo*-norbornyl	0.2		−2.8		−2.9	−3.3	−6.2	−4.2
9	2-methyl-2-propyl	0.2		−5.1		−5.2	−2.6	−7.8	−10.3
10	1-bicyclo[2.2.2]octyl	0.4		−7.0		−7.9	−1.7	−9.6	−10.3
11	4-homocubyl					(−11.2)	−1.8	−13.0	−14.6
12	cubyl					(−16.4)	−1.0	−17.4	−16.1
13	3-noradamantyl					(−16.9)	−2.7	−19.6	−17.2
14	1-homocubyl					(−26.7)	−3.0	−29.7	−29.8
15	1-norbornyl	0.6		−26.7		−27.0	−2.3	−29.3	−26.1
16	tricyclo[3.2.1.0^{3,6}]oct-6-yl					(−31.3)	−3.2	−34.5	−33.4

[a] All values in kcal mol^{-1}. [b] This work. [c] Calculated from data for chlorides. [d] Calculated from data of alcohols. [e] Calculations at HF/6-31G*. [f] Calculations with AM1.

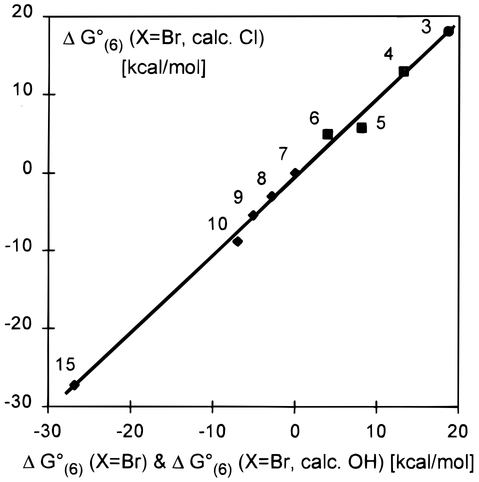

Figure 2. Plot of DPA data for chlorides with leaving group correction ($\Delta G^\circ_{(6)}$(X = Br, calcd Cl) vs DPA data for bromides, $\Delta G^\circ_{(6)}$(X = Br) and DPA data for alcohols with leaving group correction ($\Delta G^\circ_{(6)}$(X = Br, calcd OH). Slope = 0.998; intercept −0.58; $r^2 = 0.9924$; $\sigma = 1.142$.

4.3. DPA and Bridgehead Solvolysis. Figure 3 shows a correlation between the solvolysis rates and all of the DPA data presently available for bridgehead derivatives. Bromide was selected as the standard leaving group, since most of the data are available for bromides, i.e., $\Delta G^\circ_{(6)}$(X = Br). As discussed above, the data obtained for chlorides and alcohols are converted to $\Delta G^\circ_{(6)}$(X = Br, calcd Cl) and $\Delta G^\circ_{(6)}$(X = Br, calcd OH) by means of eqs 6a and 6b, respectively. Different symbols are used for the data points pertaining to different leaving groups: open squares for bromides, filled diamonds for chlorides, and filled circles for alcohols. The plot spans a rate range of ca. 23 units for log *k*. No significant or systematic deviations appear, and the data obtained with the various leaving groups are entirely consistent. The correlation line is essentially identical to that reported previously. Incorporation of the new derivatives **4**−**6** in the correlation results in a slope of 0.441. The previous conclusion, i.e., that 75−80% of the energy difference between the bridgehead derivative and the respective carbenium ion is reflected in the transition state for solvolysis, is therefore confirmed.[12] The correlation is more satisfactory than that reported in ref 12, because the new data points which fill the gap between the adamantyl derivatives **7** and 2-*tert*-butyladamantan-2-ol (**1b**) and 9-*tert*-butylbicyclo[3.3.1]nonan-9-ol (**2b**) are authentic bridgehead derivatives and not just rigid “bridgehead-like” compounds. Figure 3 reveals no significant difference in the quality of the data obtained from the different leaving groups. For this reason, average values $\Delta G^\circ_{(6)}$(X = Br, avg) will be used subsequently in the discussion whenever data for two leaving groups are available (see Table 3).

4.3.1. Solvolysis of 2-*exo*-Norbornyl Derivatives. The rate constant for solvolysis of 2-*exo*-norbornyl tosylate in 80% EtOH at 25 °C has been reported to be 2.31×10^{-4} (log $k = -3.64$).[44] Under the same conditions, 1-adamantyl tosylate solvolyzes with a rate constant of 4.03×10^{-3} (log $k = -2.39$).[45] This gives a relative rate of −1.25 for the 2-*exo*-norbornyl derivative at 25 °C. Extrapolation to 70 °C (standard reactivity scale) yields −1.08 relative to 1-adamantyl. The stability of the 2-norbornyl cation (**8e**) according to eq 6 is −2.3 kcal mol^{-1}.[12] The compound fits the plot in Figure 3 perfectly. The unusually high stability of the 2-norbornyl cation relative to that of other cations, in particular strained ones, has been noted previously.[12] It is surprising to find that the solvolysis of the 2-*exo*-norbornyl derivative proceeds in analogy to that of tertiary derivatives and that the same degree of the energy difference between R−Br and R$^+$ is expressed in the transition state of the reaction. This is plausible considering that the 2-*exo*-norbornyl derivatives should solvolyze without significant solvent participation.[45,46]

The enhanced rate for solvolysis of 2-*exo*-2-norbornyl derivatives over that of their endo epimers has been the subject of much controversy in the past.[47] While the

---

[44] Harris, J. M.; Mount, D. L.; Raber, D. J. *J. Am. Chem. Soc.* **1978**, *100*, 3139−3143.

[45] Kevill, D. N.; Kolwyck, K. C.; Weitl, F. L. *J. Am. Chem. Soc.* **1970**, *92*, 7300−7306.

[46] Bentley, T. W.; Bowen, C. T.; Morten, D. H.; Schleyer, P. v. R. *J. Am. Chem. Soc.* **1981**, *103*, 5466−5475.

[47] (a) Brown, H. C. With comments by Schleyer, P. v. R. *The Nonclassical Ion Problem;* Plenum: New York, 1977. (b) Lenoir, D.; Apeloig, Y.; Arad, D.; Schleyer, P. v. R. *J. Org. Chem.* **1988**, *53*, 661−675. (c) Grob, C. A. *Acc. Chem. Res.* **1983**, *13*, 426−431. Brown, H. C. *Acc. Chem. Res.* **1986**, *13*, 432−440. Olah, G. A.; Prakash, G. K. S.; Saunders, M. *Acc. Chem. Res.* **1983**, *13*, 440−448.

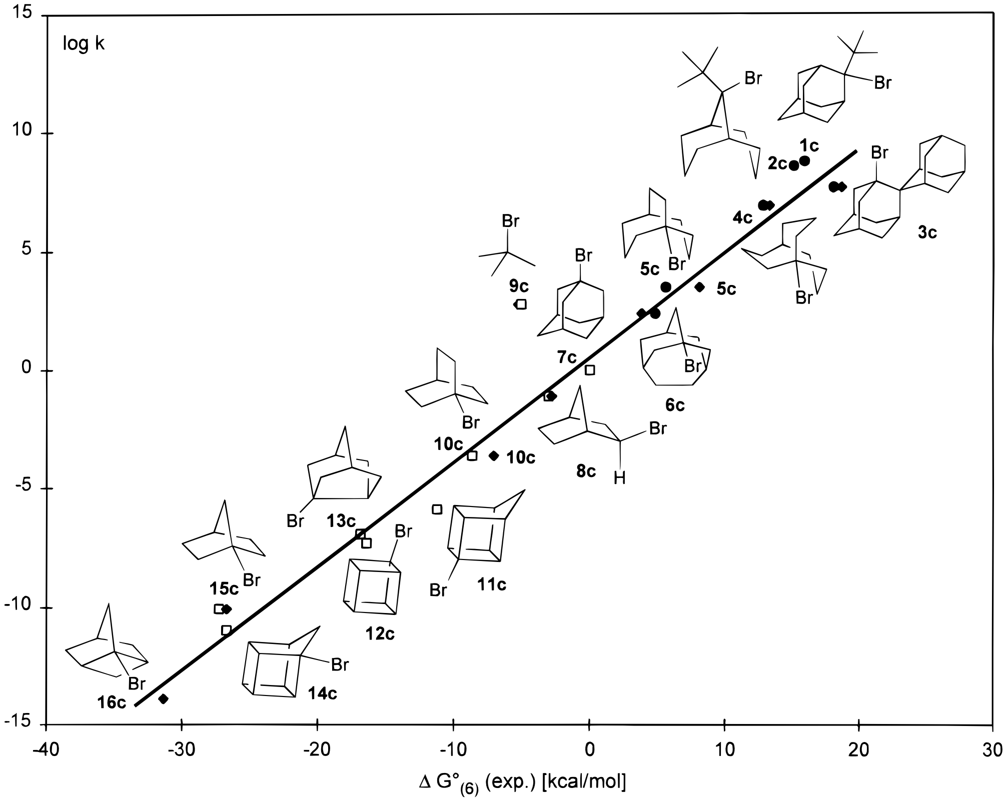

Figure 3. Plot of log *k* for bridgehead derivatives vs $\Delta G°_{(6)}$(X = Br), open squares, $\Delta G°_{(6)}$(X = Br, calcd Cl), diamonds, and $\Delta G°_{(6)}$(X = Br, calcd OH), filled circles. log $k = 0.441\Delta G°_{(6)} + 0.50$. $r^2 = 0.986$; $\sigma = 0.86$. *tert*-Butyl (**9**) excluded from correlation.

symmetrically bridged structure of the secondary 2-norbornyl cation is now established beyond reasonable doubt,[48] many questions await answers, and in particular, the structures of the transition states for 2-*exo*- and 2-*endo*-norbornyl solvolysis are not established. Schreiner et al. performed high-level ab initio calculations on these transition states using H_2O^+ as the leaving group.[49] The activation energy for the exo isomer was found to be 3.7 kcal mol^{-1} lower than that for the endo isomer, much less than the 14 kcal mol^{-1} energy difference favoring the isolated nonclassical over the classical 2-norbornyl cation. The calculations revealed that the $C_7H_{11}{}^+$ moiety of the unsymmetrically bridged exo transition state is 1.3 kcal mol^{-1} higher in energy than the fully relaxed nonclassical 2-norbornyl cation. Strong interactions between the leaving group and the developing cations compete with the stabilization by the neighboring groups and contribute significantly toward the stability of the transition state.

The implications of these results with regard to the mechanism of bridgehead solvolysis are not clear. The existence of the correlation shown in Figure 3 requires an approximately constant interaction of the leaving group with the carbon skeleton throughout the series of bridgehead transition states, including the one for 2-*exo*-norbornyl. This seems unlikely in the light of the differential leaving group interactions of the secondary exo as compared to the endo transition state, and the intervention of a compensating effect appears more likely.

4.3.2. Solvolysis of *tert*-Butyl Derivatives. The DPA data for the *tert*-butyl derivatives **9a** and **9b** [$\Delta G°_{(6)}$(X = Br) and $\Delta G°_{(6)}$(X = Cl)] satisfy the correlation depicted in Figure 2 nicely. Furthermore, the *tert*-butyl cation (**9e**) behaves perfectly well in the gas phase, and its thermodynamic stability with respect to other carbocations is well established.[12] This ion is the only significantly deviating point in Figure 3. The predicted value of Δlog k_{solv} for *tert*-butyl bromide is −2.2 log units, while the experimental value is 2.8. The difference of 5.0 log units implies an effective rate enhancement of the reaction with respect to the value expected on the grounds of the stability of the *tert*-butyl cation. The standard deviation of the fit in the correlation between Δlog k_{solv} and $\Delta G°_{(6)}$(X = Br, avg) is 0.77 log units. Hence, the experimental departure from linearity equals 6.5 times the standard deviation of fit. In statistical terms, for a system such as this, this deviation is meaningful beyond the 99% significance level.[50] At 70 °C, the rate enhancement reflects an assistance of 7.9 kcal mol^{-1} in terms of Gibbs energy of activation (1 log unit in rate constant being equivalent to 1.57 kcal mol^{-1}).

That the *tert*-butyl derivatives solvolyze faster than expected on the grounds of the stability of the *tert*-butyl cation has been recognized for some time. The *tert*-butyl cation is less stable in the gas phase than the 1-adamantyl cation, but despite this, *tert*-butyl bromide solvolyzes faster than 1-bromoadamantane. The 1-adamantyl/*tert*-butyl rate ratio decreases with the nucleophilicity of the solvent. There is general agreement that this change of the 1-adamantyl/*tert*-butyl rate ratio should be ascribed

---

(48) Olah, G. A. *Angew. Chem., Int. Ed. Engl.* **1995**, *34*, 1393−1405.

(49) Schreiner, P. R.; Severance, D. L.; Jorgensen, W. L.; Schleyer, P. v. R.; Schaefer, H. F. *J. Am. Chem. Soc.* **1995**, *117*, 2663−2664. Schreiner, P. R.; Schleyer, P. v. R.; Schaefer, H. F. *J. Org. Chem.* **1997**, *62*, 4216−1228.

(50) Massart, D. L.; Vandeginste, B. G.; Deming, S. N.; Michotte, Y.; Kaufman, L. *Chemometrics: a Textbook*; Elsevier: Amsterdam, 1988; Chapter 5, pp 72−92.

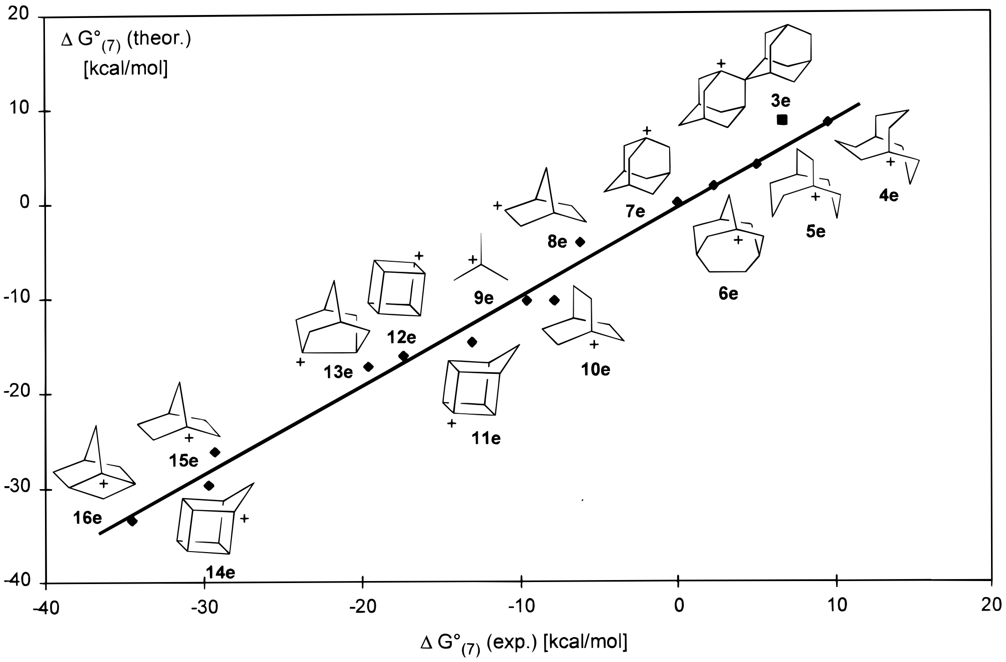

Figure 4. Calculated (MP2/6-311G**) vs experimental standard Gibbs energy changes for hydride tranfer (reaction 7). $\Delta G°_{(7)}$ (theor) = $0.94\Delta G°_{(7)}$(exptl) − 0.54. $r^2 = 0.9885$; $\sigma = 1.48$.

to nucleophilic solvent participation in the case of the *tert*-butyl derivative, a pathway precluded for bridgehead derivatives.[51] We have recently proposed that part of this rate enhancement should be attributed to the decreased amount of charge development in the transition state for solvolysis in the condensed phase as compared to that of free ions in the gas phase.[9,10] The recent theoretical calculations of Schreiner et al.[49] lend some indirect support to this hypothesis: the transition state for solvolysis is stabilized by interactions of the reactive center with the molecular skeleton of the substrate that compete with those of the leaving group. In the case of the *tert*-butyl derivative, stabilization by the skeleton is limited owing to the small number of atoms present. In contrast, strong interactions with the leaving group may provide additional stabilization of the transition state and, thereby, account for the high reactivity of the *tert*-butyl in comparison to bridgehead derivatives.

4.4. DPA and Theoretical Ion Stabilities. The DPA results may be linked to theoretically calculated hydride transfer thermodynamics. As in ref 12, values of $\Delta G°_{(7)}$ defined by eq 7 are obtained from the experimental data $\Delta G°_{(6)}$(X = Br, avg) and the computed (HF/6-31G*) leaving group correction for replacement of the bromo substituent by hydrogen, $\Delta G°_{(6c)}$, according to reaction 6c.

$$\mathrm{R^+(g) + Ad{-}H(g) \rightarrow R{-}H(g) + Ad^+(g)} \quad \Delta G°_{(7)} \qquad (7)$$

$$\mathrm{R{-}X(g) + Ad{-}H(g) \rightarrow R{-}H(g) + Ad{-}X(g)} \quad \Delta G°_{(6c)} \qquad (6c)$$

The theoretical calculations for hydride transfer were carried out at the MP2/6-311G** level to generate values for $\Delta G°_{(7)}$(theor). The details of the calculations are collected in Tables 2 and 3. The results for the relevant quantities are summarized in Table 3 and are presented in Figure 4.

Comparison of the two sets of data reveals almost perfect agreement between experimental and calculated energies for hydride transfer for the bridgehead series. Even the *tert*-butyl cation is well behaved with respect to hydride transfer, although its solvolysis rate constant deviates seriously in Figure 3. This agreement between experiment and theory provides strong support for the reliability of the DPA method. The successful correlation of the rate constants for solvolysis with the DPA data over the full rate range for bridgehead derivatives confirms the original hypothesis that in the bridgehead series the rate constants for solvolysis are determined by the stability of the bridgehead carbenium ion relative to its precursor.

5. Conclusions

The existence of a linear correlation between bridgehead solvolytic reactivity and stability of bridgehead carbenium ions was proposed more than 25 years ago. At that time, the stability of carbenium ions and that of their precursors was evaluated in terms of steric strain, which, in turn, was calculated by an empirical model. In the present work, the stability of bridgehead carbenium ions relative to that of their precursors is determined experimentally, and the significance of the experimental data is confirmed by high level ab initio calculations. The correlation between bridghead solvolytic reactivity in the condensed phase and gas-phase ion stability holds over a rate range of 23 log units, which is truly remarkable. This confirms the original hypothesis that bridgehead derivatives solvolyse by a common mechanism and that the stability of the intermediate carbenium ions is reflected in the transition state of the reaction. Bridgehead solvolysis may, therefore, be considered as a mecha-

---

(51) Fainberg, A. H.; Winstein, S. *J. Am. Chem. Soc.* **1957**, *79*, 1602−1608. Fry, J. L.; Harris, M. J.; Bingham, R. C.; Schleyer, P. v. R. *J. Am. Chem. Soc.* **1970**, *92*, 2540−2542. Raber, D. J.; Bingham, R. C.; Harris, J. M.; Fry, J. L.; Schleyer, P. v. R. *J. Am. Chem. Soc.* **1970**, *92*, 5977−5981. Bentley, T. W.; Carter, G. E. *J. Am. Chem. Soc.* **1982**, *104*, 5741−5747.

nistic model for unimolecular substitution reactions proceeding without nucleophilic solvent participation, and deviations from bridgehead behavior point out mechanistic changes.

Acknowledgment. This work was supported by the Spanish DGICYT (Grant No. PB96-0927-CO2-01), the French CNRS, and the Swiss National Science Foundation (Grant Nos. 20-52581.97 and 21-45790.95). We are grateful for the generous allocation of computer time provided by the Swiss Center of Scientific Computing, and thanks are due to C. Chiancone for help in data processing.

JO990724X